Defects in Heavy-Fermion Materials: Unveiling Strong Correlations in Real Space

Jeremy Figgins and Dirk K. Morr

Department of Physics, University of Illinois at Chicago, Chicago, Illinois 60607, USA

(Received 27 October 2010; published 2 August 2011)

Defects provide important insight into the complex electronic and magnetic structure of heavy-fermion materials by inducing qualitatively different real-space perturbations in the electronic and magnetic correlations of the system. These perturbations possess direct experimental signatures in the local density of states, such as an impurity bound state, and the nonlocal spin susceptibility. Moreover, highly nonlinear quantum interference between defect-induced perturbations can drive the system through a first-order phase transition to a novel inhomogeneous ground state.

DOI: 10.1103/PhysRevLett.107.066401 PACS numbers: 71.27.+a, 75.20.Hr, 75.30.Mb

Heavy-fermion materials exhibit a plethora of puzzling phenomena which are believed to arise from the competition [1] between Kondo screening [2] and antiferromagnetic ordering. Of particular interest are the non-Fermi-liquid properties [3] observed in the quantum critical region of the heavy-fermion phase diagram, whose microscopic origin is still a topic of debate [4–8]. Recent ground-breaking scanning tunneling spectroscopy (STS) experiments [9–11] have shed light on this debate by providing insight into the electronic and magnetic structure of heavy-fermion materials, in particular, through quasiparticle interference spectroscopy [9] which utilizes the effects of defects. These results raise the interesting question of whether, similar to the high-temperature superconductors [12], defects can be employed in heavy-fermion materials to disentangle and spatially resolve their electronic and magnetic structure.

In this Letter, we demonstrate that defects in heavy-fermion materials provide an unprecedented opportunity to differentiate (in real space) between electronic correlations arising from Kondo screening, and antiferromagnetic correlations between the magnetic moments. In particular, defects [13,14] induce perturbations in the electronic and magnetic structure that exhibit characteristically different spatial patterns and possess experimental signatures in the local density of states (LDOS) of the conduction band, and the nonlocal f-electron spin susceptibility, respectively. The spatial extent of these perturbations grows with the strength of the magnetic interactions, and thus directly reflects the degree of correlations. Moreover, nonmagnetic impurities can induce an impurity bound state, in contrast to defects in the form of missing magnetic (Kondo) atoms. Finally, we show that the strongly correlated nature of these materials manifests itself in highly nonlinear quantum interference effects between defects that can drive the system through a first-order phase transition to a novel inhomogeneous ground state. Our findings demonstrate that defects provide unique insight into the competing interactions in heavy-fermion materials, thus presenting a new approach to solving the complex heavy-fermion problem.

The starting point for our study is the Kondo-Heisenberg Hamiltonian [5–8]

$$\mathcal{H} = -t \sum_{\langle \mathbf{r},\mathbf{r}'\rangle,\alpha} c^\dagger_{\mathbf{r},\alpha} c_{\mathbf{r}',\alpha} - \mu \sum_{\mathbf{r},\alpha} c^\dagger_{\mathbf{r},\alpha} c_{\mathbf{r},\alpha} + \frac{J}{2} \sum_{\mathbf{r},\alpha,\beta} \mathbf{S}^K_{\mathbf{r}} \cdot c^\dagger_{\mathbf{r},\alpha} \boldsymbol{\sigma}_{\alpha\beta} c_{\mathbf{r},\beta} + \sum_{\mathbf{r},\mathbf{r}'} I_{\mathbf{r},\mathbf{r}'} \mathbf{S}^K_{\mathbf{r}} \cdot \mathbf{S}^K_{\mathbf{r}'}. \quad (1)$$

With nearest-neighbor hopping $t = 0.5E_0$ and chemical potential $\mu = -1.809E_0$ (E_0 is an overall energy scale), one obtains a Fermi wavelength $\lambda_F^c = 10a_0$ (a_0 is the lattice constant) of the (decoupled) conduction band with electron density $n_c = 0.062$. $c^\dagger_{\mathbf{r},\alpha}$ ($c_{\mathbf{r},\alpha}$) creates (annihilates) a conduction electron with spin α at site $\mathbf{r}$. $J > 0$ is the Kondo coupling, and $\mathbf{S}^K_{\mathbf{r}}$ is the $S = 1/2$ spin operator of the magnetic (Kondo) atom. $I_{\mathbf{r},\mathbf{r}'}$ is the antiferromagnetic coupling between nearest-neighbor Kondo atoms. Its microscopic origin, direct exchange [6,7] or RKKY-interaction [1,5,8], is in general not known. However, since it is irrelevant for the purpose of this study, we consider I and J to be independent parameters, in accordance with earlier work [6,7]. Finally, the conduction band and magnetic atoms possess identical square lattices with $\mathbf{r}$ representing the location of a Kondo atom and the conduction band site that it couples to.

In the *large-N* approach [15–18], $\mathbf{S}^K_{\mathbf{r}}$ is represented by pseudofermion operators, $f^\dagger_{\mathbf{r},m}$, $f_{\mathbf{r},m}$, that obey the constraint $\hat{n}_f(\mathbf{r}) = \sum_{m=1,\ldots,N} f^\dagger_{\mathbf{r},m} f_{\mathbf{r},m} = 1$ for all $\mathbf{r}$ with $N = 2$ being the number of fermionic flavors for a spin operator with $S = 1/2$. In order to decouple the resulting Hamiltonian, we introduce the mean fields

$$s(\mathbf{r}) = \frac{J}{2} \sum_\alpha \langle f^\dagger_{\mathbf{r},\alpha} c_{\mathbf{r},\alpha} \rangle; \quad \chi(\mathbf{r},\mathbf{r}') = \frac{I_{\mathbf{r},\mathbf{r}'}}{2} \sum_\alpha \langle f^\dagger_{\mathbf{r},\alpha} f_{\mathbf{r}',\alpha} \rangle. \quad (2)$$

Here, a nonzero local hybridization $s(\mathbf{r})$ between the conduction electron and the magnetic f-electron states describes the screening of a magnetic moment, and the magnetic bond variable $\chi(\mathbf{r},\mathbf{r}')$ represents the antiferromagnetic (spin-liquid) correlations [6,7] between nearest-neighbor moments. By adding the term $\sum_{\mathbf{r},\alpha} \varepsilon_f(\mathbf{r}) f^\dagger_{\mathbf{r},\alpha} f_{\mathbf{r},\alpha}$

to the Hamiltonian, the constraint $\langle \hat{n}_f(\mathbf{r}) \rangle = 1$ can be enforced through the on-site energy $\varepsilon_f(\mathbf{r})$ [19,20]. The resulting quadratic Hamiltonian can be diagonalized in real space [assuming periodic boundary conditions for an $(M \times M)$ lattice], allowing a self-consistent calculation of $s(\mathbf{r})$, $\chi(\mathbf{r}, \mathbf{r}')$, and $\varepsilon_f(\mathbf{r})$. We study systems well inside the Kondo screened regime where $s(\mathbf{r}) \neq 0$ for all sites and fluctuation corrections beyond the mean-field level are expected to be weak [7,16]. Moreover, a missing Kondo atom at site $\mathbf{R}$, a *Kondo hole*, is described by removing the spin operator $\mathbf{S}^K_{\mathbf{R}}$ from the above Hamiltonian [19]. Similarly, replacing a magnetic atom by a nonmagnetic one corresponds to removing $\mathbf{S}^K_{\mathbf{R}}$ from the Hamiltonian and adding the scattering term $U_0 \sum_\alpha c^\dagger_{\mathbf{R},\alpha} c_{\mathbf{R},\alpha}$. We consider lattices with $M = 41$ since the mean-field parameters change only weakly ($\leq 0.5\%$) for $M > 41$. For a clean system, our formalism reproduces the mean-field results of the lattice Kondo-Heisenberg Hamiltonian [6,7,17].

We begin by considering the case of a Kondo hole located at $\mathbf{R} = (0, 0)$. In Figs. 1(a) and 1(b) we present spatial plots of the relative change in the hybridization, Δs, and the conduction electron density, Δn_c, respectively, between the Kondo lattice with and without a hole. Both quantities exhibit similar spatial oscillations, whose isotropy and wavelength of $\lambda^c_F/2$ imply that they are determined by the Fermi surface of the unhybridized conduction band [Fig. 1(d)]. The oscillations in Δs and Δn_c decay exponentially and change only very weakly with I/J. However, their decay length, ξ_s, increases approximately linearly with s^{-1} of the clean system [21]. In contrast, the spatial oscillations of $\Delta\chi$ shown in Fig. 1(c) extend predominantly along the lattice diagonal. They reflect the strongly anisotropic Fermi surface of the hybridized system [see Fig. 1(d)], which possesses a large degree of nesting and a Fermi velocity, v_1, along the lattice diagonal which is about 10 times larger than that along the bond direction, v_2. Thus, the oscillations of $\Delta\chi$ possess a wavelength of $\lambda^h_F/2 = \sqrt{2}a_0$, with λ^h_F being the Fermi wavelength of the hybridized Fermi surface along the diagonal. The envelope of these oscillations decays exponentially away from the Kondo hole with a decay length, ξ_χ, that increases approximately linearly with I/J [21]. This dependence is expected since a Kondo hole can be mapped onto a localized state outside the conduction band whose effects on $\Delta\chi$ or Δs necessarily decay exponentially. Moreover, since the amplitude and spatial extent of $\Delta\chi$ increase with I/J, $\Delta\chi$ is a direct measure for the strength of the magnetic interaction. A weaker reflection of these anisotropic oscillations can also be found in Δs, demonstrating the coupling between the system's electronic and magnetic degrees of freedom. Finally, we note that the relation between the spatial structure of Δs and $\Delta\chi$ and the form of the unhybridized and hybridized Fermi surfaces, respectively, holds for all parameters of n_c and J that we have considered so far [21].

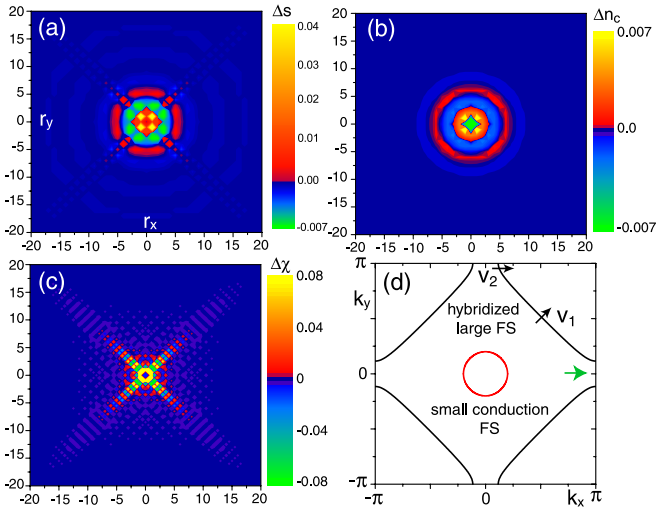

FIG. 1 (color online). Kondo hole system for $J = E_0$ and $I/J = 0.001$. Contour plots of (a) Δs, (b) Δn_c, and (c) $\Delta\chi(\mathbf{r}, \mathbf{r}')$ [shown at $(\mathbf{r} + \mathbf{r}')/2$]. (d) Large Fermi surface (black lines) of the unperturbed Kondo lattice (with $s = 0.0485E_0$, $\chi = 0.000166E_0$ and $\varepsilon_f = 0.000123E_0$) arising from the hybridization of the f-electron and conduction bands and the small [red (gray) line] Fermi surface of the unhybridized conduction band.

The spatial perturbations in $s(\mathbf{r})$ possess a direct spectroscopic signature in the LDOS of the conduction band, $N_c(\mathbf{r}, \omega)$, which can be probed via STS [22,23]. $N_c(\mathbf{r}, \omega)$ for an unperturbed Kondo lattice [see Fig. 2(a)] exhibits a hybridization gap which was recently observed in STS experiments [9–11]. The peak in the LDOS at the low-energy side of the gap arises from the van Hove singularity of the hybridized Fermi sea [green (light gray) arrow in Fig. 1(d)]. In comparison, the LDOS at the site of the Kondo hole, $\mathbf{R}$, shows a significant redistribution of spectral weight from negative to positive energies. To understand this effect, we note that the screening of a single Kondo atom leads to an increase in the local electron density, $n_c(\mathbf{r}) = \int_{-\infty}^{\infty} d\omega n_F(\omega) N_c(\mathbf{r}, \omega)$, with n_F being the Fermi function, and hence a shift of spectral weight in

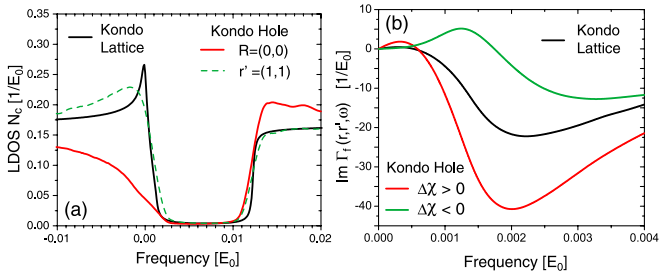

FIG. 2 (color online). (a) $N_c(\mathbf{r}, \omega)$ for the unperturbed Kondo lattice, and in the Kondo hole system at $\mathbf{R} = (0, 0)$, and $\mathbf{r}' = (1, 1)$ where $\Delta s(\mathbf{r}') > 0$. (b) The nonlocal f-electron spin susceptibility, $\Gamma_f(\mathbf{r}, \mathbf{r}', \omega)$ between nearest-neighbor sites in the unperturbed Kondo lattice, and in the Kondo hole system between sites $\mathbf{r} = (1, 0)$ and $\mathbf{r}' = (1, 1)$ with $\Delta\chi > 0$ and between sites $\mathbf{r} = (1, 1)$ and $\mathbf{r}' = (1, 2)$ with $\Delta\chi < 0$.

$N_c(\mathbf{r}, \omega)$ from positive to negative energies. A Kondo hole leads to the opposite effect with a decrease in $n_c(\mathbf{R})$, and the corresponding changes in N_c shown in Fig. 2(a). Moreover, since for a site with $\Delta s(\mathbf{r}) > 0$ one has $\Delta n_c(\mathbf{r}) > 0$ [cf. Figs. 1(a) and 1(b)], the concomitant redistribution of spectral weight in $N_c(\mathbf{r}, \omega)$ is a direct measure of $\Delta s(\mathbf{r})$. The form of $N_c(\mathbf{r}', \omega)$ at the next-nearest-neighbor site of the Kondo hole [see Fig. 2(a)] with $\Delta s(\mathbf{r}') > 0$, exhibits an increase in spectral weight at negative frequencies, and hence confirms this conclusion. Note that the (positive) spatial correlation between Δs and Δn_c for $n_c < 1$ [Figs. 1(a) and 1(b)] turns into an anticorrelation for $n_c > 1$ [22]. Moreover, the spatial oscillations in $\chi(\mathbf{r}, \mathbf{r}')$ possess a direct spectroscopic signature in the nonlocal f-electron spin susceptibility, $\Gamma_f(\mathbf{r}, \mathbf{r}', \omega)$. In particular, for nearest-neighbor sites, $\mathbf{r}$, $\mathbf{r}'$, with $\Delta\chi > 0$ ($\Delta\chi < 0$), $|\mathrm{Im}\Gamma_f|$ is enhanced (suppressed) in comparison to the unperturbed Kondo lattice [see Fig. 2(b)]. These effects are expected to be observable in the near future [24,25] via nuclear magnetic resonance techniques [26] or nanoscale magnetic resonance spectroscopy [27].

The replacement of a Kondo atom at $\mathbf{R} = (0, 0)$ by a nonmagnetic impurity with an attractive scattering potential, $U_0 < 0$, leads to a form of Δs, Δn_c, and $\Delta\chi$ [Figs. 3(a)–3(c)] that possesses distinct differences to those induced by a Kondo hole. Specifically, it causes a sign change of Δn_c, i.e., a site with $\Delta n_c < 0$ for the Kondo hole case, now has $\Delta n_c > 0$ [cf. Figs. 1(b) and 3(b)]. Since the same change also occurs in Δs and $\Delta\chi$, it follows that the electronic and magnetic correlations are strongly affected by the spatial redistribution of n_c. When the magnitude of $U_0 < 0$ exceeds a threshold value, $|U_c|$, an *impurity bound state* is formed around the impurity. Its spectroscopic signature is a sharp peak in $N_c(\mathbf{r}, \omega)$ inside the hybridization gap [see Fig. 3(d)]. With increasing $|U_0|$, the bound state first emerges at the high energy side of the hybridization gap and then moves to lower energies [see Fig. 3(d)]. The bound state is spatially isotropic, and decays exponentially away from the impurity with a decay length, $\xi_D \approx 0.65 a_0$ [see Fig. 3(e)]. This small value of ξ_D demonstrates that the bound state is predominantly formed by f-electrons since a state arising from conduction electrons would have $\xi_D \gtrsim 60 a_0$ due to the significantly larger v_F. The f-electron nature of the bound state is also expected since with increasing $|U_0|$, it is pulled into the hybridization gap from states located at the gap edges, which are f-electron-like in nature [22]. It also directly reflects the strong correlations between the light and heavy bands since it is induced by impurity scattering of conduction electrons only. In contrast, the spatial oscillations of $N_c(\mathbf{r}, \omega)$ for frequencies outside the hybridization gap are delocalized [see Fig. 3(f)], and hence arise from conduction electrons. The existence of a nonzero U_c, whose sign and magnitude are determined by the particle-hole asymmetry of the conduction band (here, $U_c = -0.62 E_0$), might explain the disparate physical properties of

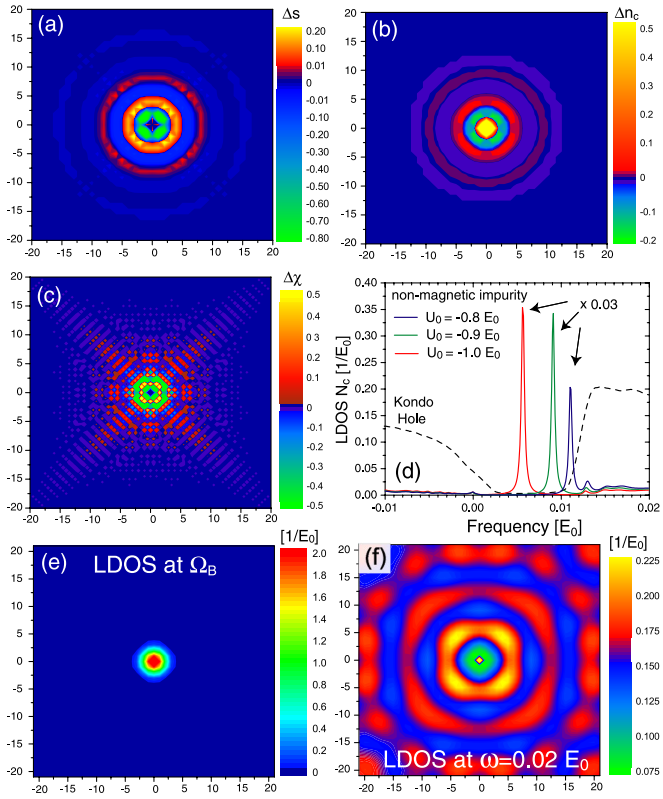

FIG. 3 (color online). Kondo lattice with a nonmagnetic impurity at $\mathbf{R} = (0, 0)$ and $U_0 = -1.0 E_0$, $I/J = 0.001$. Contour plot of (a) Δs, (b) Δn_c, and (c) $\Delta\chi$. (d) $N_c(\mathbf{R}, \omega)$ showing the existence of an impurity bound state. Contour plot of $N_c(\mathbf{r}, \omega)$ at (e) $\omega = \Omega_B$, and (f) outside the hybridization gap at $\omega = 0.02 E_0$.

heavy-fermion materials containing different types of nonmagnetic impurities [13]. Moreover, for a system with a soft hybridization gap [22,28], the bound state transforms into a resonant state, and U_c becomes a crossover scale [21]. Finally, our description of a nonmagnetic impurity, and the nature of the induced bound state, differ qualitatively from previous work [29] where the impurity was modeled as a Kondo atom with $\varepsilon_f(\mathbf{R}) \to \infty$ but $s(\mathbf{R}) \neq 0$. Within our theoretical model, these assumptions are inconsistent, since $\varepsilon_f(\mathbf{R}) \to \infty$ necessarily implies $s(\mathbf{R}) \to 0$.

The strongly correlated nature of the Kondo lattice leads to highly nonlinear quantum interference of the spatial perturbations emanating from adjacent Kondo holes. For a periodic array of Kondo holes embedded in the Kondo lattice, this nonlinearity leads to a first-order phase transition with increasing I into a novel inhomogeneous ground state. The kink in the free energy at I_c, shown in Fig. 4(a) demonstrates the first-order nature of this transition (here, we consider a square lattice of Kondo holes separated by $a_H = 41 a_0$). The phase transition occurs, when the spatial perturbations in χ, whose spatial extent increases with I, reach the corners of the unit cell in a Kondo hole array, where they interfere with each other nonlinearly and drive the system through a first-order

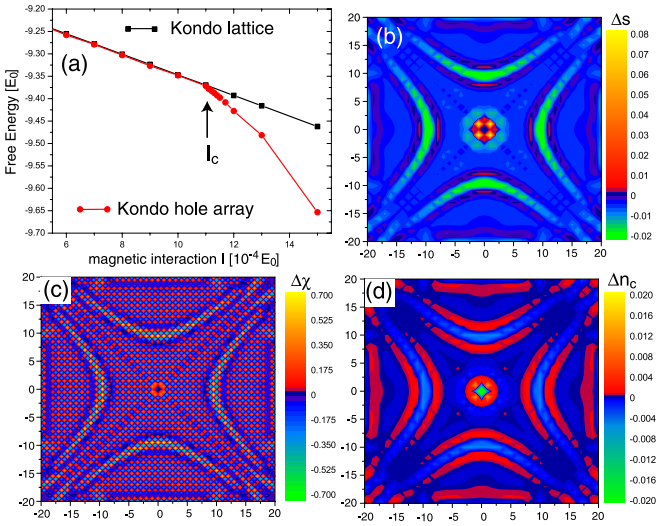

FIG. 4 (color online). (a) Free energy of the unperturbed Kondo lattice and Kondo hole array as a function of I/J. Contour plots of (b) Δs, (c) $\Delta\chi$, and (d) Δn_c for one unit cell of the Kondo hole array and $I/J = 0.0013 > I_c/J = 0.0011$.

transition. The spatial patterns of Δs, $\Delta\chi$, and Δn_c for $I > I_c$ shown in Figs. 4(b)–4(d) are strikingly different from the ones for $I < I_c$ (see Fig. 1), and reflect the highly inhomogeneous nature of this state. The similarity of the patterns for $I > I_c$ and the large amplitude of Δn_c, suggest that while the phase transition is driven by quantum interference between perturbations in χ, the resulting real-space patterns are determined by the redistributed conduction electron density.

In summary, we demonstrated that defects induce qualitatively different spatial patterns of Δs and $\Delta\chi$, which provide important insight into the complex electronic and magnetic structure of heavy-fermion materials. Moreover, nonmagnetic impurities can induce qualitatively different effects from those of Kondo holes, such as an impurity bound state. Finally, strong correlations give rise to nonlinear quantum interference effects that can drive the system through a first order phase transition to a highly inhomogeneous ground state.

We would like to thank E. Abrahams, J. C. Davis, P. C. Hammel, H. Manoharan, S. Sachdev, Q. Si, F. Steglich and H. v. Lohneysen for stimulating discussions. D. K. M. would like to thank the Aspen Center for Physics and the James Franck Institute at the University of Chicago for its hospitality during various stages of this project. This work is supported by the U.S. Department of Energy under Award No. DE-FG02-05ER46225.

Note added.—Recently, STS experiments by Hamidian *et al.* [30] on Th-doped URu_2Si_2 confirmed the predicted existence of spatial hybridization oscillations [with a wave vector twice that of the (unhybridized) conduction band, see Fig. 1(a)], and of an impurity bound state [see Fig. 3(d)] [29]. The experimental confirmation of our predictions represents a significant advance towards understanding the complex electronic and magnetic structure of heavy-fermion materials in general, and of disorder effects in particular [13,14].

[1] S. Doniach, Physica (Amsterdam) **91B** , 231 (1977).
[2] J. Kondo, Prog. Theor. Phys. **32**, 37 (1964).
[3] M. B. Maple *et al.*, J. Low Temp. Phys. **99**, 223 (1995); A. Schroder *et al.*, Nature (London) **407**, 351 (2000); G. R. Stewart, Rev. Mod. Phys. **73**, 797 (2001); J. Custers *et al.*, Nature (London) **424**, 524 (2003); H. von Lohneysen *et al.*, Rev. Mod. Phys. **79**, 1015 (2007); P. Gegenwart *et al.*, Nature Phys. **4**, 186 (2008).
[4] P. Coleman *et al.*, J. Phys. Condens. Matter **13**, R723 (2001); P. Sun and G. Kotliar, Phys. Rev. Lett. **91**, 037209 (2003).
[5] Q. M. Si *et al.*, Nature (London) **413**, 804 (2001).
[6] T. Senthil, S. Sachdev, and M. Vojta, Phys. Rev. Lett. **90**, 216403 (2003).
[7] I. Paul, C. Pepin, and M. R. Norman, Phys. Rev. Lett. **98**, 026402 (2007).
[8] P. Coleman, in *Handbook of Magnetism and Advanced Magnetic Materials*, edited by H. Kronmüller and S. Parkin (Wiley and Sons, New York, 2007).
[9] A. R. Schmidt *et al.*, Nature (London) **465**, 570 (2010).
[10] P. Aynajian *et al.*, Proc. Natl. Acad. Sci. U.S.A. **107**, 10383 (2010).
[11] S. Ernst *et al.*, Nature (London) **474**, 362 (2011).
[12] A. Yazdani *et al.*, Phys. Rev. Lett. **83**, 176 (1999); E. W. Hudson *et al.*, Science **285**, 88 (1999); A. V. Balatsky, I. Vekhter, and J. X. Zhu, Rev. Mod. Phys. **78**, 373 (2006).
[13] F. Steglich *et al.*, Physica (Amsterdam) **148B**, 6 (1987).
[14] C. L. Lin *et al.*, Phys. Rev. Lett. **58**, 1232 (1987); A. Lopez de la Torre *et al.*, Physica (Amsterdam) **179B**, 208 (1992); J. M. Lawrence *et al.*, Phys. Rev. B **53**, 12 559 (1996).
[15] A. D. Hewson, *The Kondo Problem to Heavy Fermions* (Cambridge University Press, Cambridge, 1997).
[16] N. Read and D. Newns, J. Phys. C **16**, 3273 (1983).
[17] P. Coleman, Phys. Rev. B **28**, 5255 (1983).
[18] N. E. Bickers, Rev. Mod. Phys. **59**, 845 (1987).
[19] R. K. Kaul and M. Vojta, Phys. Rev. B **75**, 132407 (2007).
[20] J. R. Iglesias, C. Lacroix, and B. Coqblin, Phys. Rev. B **56**, 11 820 (1997).
[21] J. Figgins and D. K. Morr (unpublished).
[22] J. Figgins and D. K. Morr, Phys. Rev. Lett. **104**, 187202 (2010).
[23] M. Maltseva, M. Dzero, and P. Coleman, Phys. Rev. Lett. **103**, 206402 (2009); P. Wölfle, Y. Dubi, and A. V. Balatsky, Phys. Rev. Lett. **105**, 246401 (2010).
[24] H. Alloul (private communication).
[25] P. C. Hammel (private communication).
[26] H. Alloul *et al.*, Rev. Mod. Phys. **81**, 45 (2009).
[27] P. C. Hammel, Nature (London) **458**, 844 (2009).
[28] T. Yuan, J. Figgins, and D. K. Morr, arXiv:1101.2636.
[29] R. Freytag, and J Keller, Z. Phys. B **80**, 241 (1990); R. Sollie and P. Schlottmann, J. Appl. Phys. **69**, 5478 (1991).
[30] M. H. Hamidian *et al.* (to be published).